DOI: 10.1002/zaac.200700440

Preparation, Crystal Structure, Physical Properties and Electronic Band Structure of $TlScQ_2$ (Q = S, Se and Te)

Christoph L. Teske[a], Wolfgang Bensch[a,*], Sergey Mankovsky[b], and Hubert Ebert[b]

[a] Kiel, Institut für Anorganische Chemie, Christian-Albrechts-Universität
[b] München, Department Chemie und Biochemie − Physikalische Chemie, Ludwig-Maximilians-Universität

Received July 11th, 2007.

Abstract. The title compounds were prepared by reaction of Tl_2Q (Q = S, Se and Te) Sc and Q in the temperature range of 200 to 500 °C. The structures of the selenide and the telluride adopt the α-$NaFeO_2$ type, while $TlScS_2$ crystallizes in the β-$RbScO_2$ type structure. The space group is $R\bar{3}m$ for $TlScSe_2$ and $TlScTe_2$ with a = 3.9370(4) Å, c = 23.194(5) Å, and a = 4.2129(4) Å, c = 24.099(3) Å, respectively. The sulphide crystallizes in $P6_3/mmc$ with a = 3.761(3) Å and c = 14.942(4) Å. The crystal chemical relations between the three chalcogenides are discussed. According to the electrical measurements and the band structure calculations, the compounds are semiconductors or poor metals.

Keywords: Thallium; Scandium; Chalcogenides; Crystal structure; Electronic band structure

Introduction

Among the simply composed ternary compounds rare earth chalcogenides like $ALnQ_2$ (A = alkaline metal, Ln = lanthanoid and Q = S, Se, Te) are subject of interest e. g. because of the possible coupling of magnetic moments in these structures and the resulting practical applications. The first compounds with A = Li, Na, and K were prepared by *Ballestracci* and *Bertaut* [1, 2], sulphides and selenides with A = Li by *Ohtani* et al. [3]. The series of compounds $NaLnS_2$ (Ln = Ho, Er, Tm and Lu) were reported by *Schleid* and *Lissner* [4]. Sato et al. also reported on $NaLnS_2$ (Ln = La, Nd, Pr and Gd) [5, 6]. Further extensive investigations were undertaken by *Bronger* et al. (A = Rb and Cs) [7−9]. *Plug* and *Verschoor* determined the structure of $KCeS_2$ [10, 11], and $KErTe_2$ was investigated by *Keane* and *Ibers* [12]. More recent investigations were carried out by *Deng* et al. on $RbLnSe_2$ (Ln = La to Er and Lu) [13]. *Stöwe* intensively investigated the tellurides $ALnTe_2$ (with A = K, Rb, Cs and Ln = La, Pr, Gd; Ce, Nd and Nd) [14]. The crystal structure of $KYbSe_2$ was determined by *Gray*, *Martin* and *Dorhout* [15], and *Deng* and *Ibers* recently published their results on $CsYbSe_2$ [16].

Among these over hundred compounds the most commonly adopted structure is the α-$NaFeO_2$ type. Some materials with A = Li or Na [1−3, 5] exhibit disordered structures which adopt the rock-salt type. An additional exception is $NaPrTe_2$ [17], which crystallizes in a new cubic form. A few sulfides like $CsLnS_2$ are reported in a hexagonal modification forming the β-$RbScO_2$ type structure [18], which is also observed for $CsYbSe_2$ [16]. This is accompanied by a slight distortion of the octahedral surrounding of the A^+ cation in the α-$NaFeO_2$ type towards a trigonal-prismatic coordination and can be discussed in connection with the ratio R of ionic radii (R = $r(Ln^{3+})/r(A^+)$) [14], which amounts to 0.52 for $CsYbSe_2$ (with $r(Yb^{3+})$ = 0.868 and $r(Cs^{1+})$ = 1.67 Å [19]). These observations indicate a rough relation between chemical composition, atomic volume and possible crystal structures. A similar trend should be observed for homologous chalcogenides ABQ_2 composed of the same A and B cation resulting in an identical ratio R of the ionic radii r but containing different Q atoms (Q = S, Se or Te). For instance, the substitution of Se for S is accompanied by a reduction of the partial molar volume and this may be viewed as an increase of the so-called "chemical pressure". This could induce a slight distortion necessary for stabilising the β-$RbScO_2$ type structure. In this context application of external pressure seems also likely to have the same influence. To learn more about this hypothesis we selected the homologous compounds $TlScQ_2$ (Q = S, Se, Te) having a very similar value of R = 0.5 (with $r(Sc^{3+})$ = 0.745 and $r(Tl^{1+})$ = 1.5 Å [19]) as $CsYbSe_2$. Here we report on the preparation, crystal structures, physical properties and electronic band structure of the series $TlScQ_2$ (Q = S, Se, Te).

Experimental Section

a) Preparation

Starting materials were the elements Tl (99.99 % Johnson Matthey), Sc (Stanford Materials Corporation 99.999 %), S (sublimed), Se (Riedel-De Haën 99.5 %) and Te (Fluka 99.7 %). Tl_2S was prepared by decomposition of Tl_2CS_3 as described elsewhere [20]. Tl_2Se and Tl_2Te were synthesized from the elements in sealed glass

* Prof. Dr. W. Bensch
Inst. f. Anorg. Chemie der Universität
Otto-Hahn-Platz 6/7
D-24098 Kiel
E-mail: wbensch@ac.uni-kiel.de

ampoules (DURAN®) under reduced Ar-pressure (p ≅ 8 mbar) in the temperature rage of 200 to 500 °C. The ternary compounds $TlScQ_2$ (with Q = S, Se and Te) were prepared by solid-state-reaction from stoichiometric mixtures of Tl_2Q and the elements in a sequence of several steps always in sealed ampoules under reduced Ar-pressure.

1. The mixtures were heated slowly (3 K/min) to T ≈ 500 °C and the temperature kept for 18 to 24 h. After the heat treatment the initial melt of Tl chalcogenides had solidified and the ampoules (DURAN®) were taken out of the furnace.

2. The samples were homogenized and heated again at T ≈ 530 °C (in DURAN®) for at least one day.

3. Progress of reaction was controlled by X-Ray powder diffraction (SIEMENS D5000 diffractometer, Cu $K\alpha_1$ λ = 1.54056 Å). Step 2 was repeated until no reflections of the starting materials could be detected in the patterns (Fig 1.) Finally micro-crystalline powders of $TlScS_2$ (dark brown), $TlScSe_2$ (black) and $TlScTe_2$ (black) were obtained. The samples are stable in dry air for a long period.

4. Single crystals for X-Ray structure investigation were grown in sealed silica glass ampoules in Ar atmosphere during a heating period of at last one week in the temperature range of T ≈ 800 to 840 °C without any surplus of chalcogen.

An excess of chalcogen might lead to decomposition at these elevated temperatures, which was quite obvious for $TlScS_2$ where Tl_2S_x condensed at the colder parts of the ampoule and yellow-orange Sc_2S_3 was detected in the residue of the sample.

b) Electrical conductivity

For electrical measurements sintered (argon atmosphere, T about 470 °C, 3 d) pellets of polycrystalline $TlScQ_3$ (diameter ≈ 8 mm, thickness ≈ 2 mm) were used. Contacts were made with silver conducting paste. The resistance was recorded in the temperature range 20 K ≤ T ≤ 300 K applying the four-probe method in the dc mode [21].

c) Single crystal X-ray investigations

The intensity data for single crystal X-ray investigations were collected on a STOE AED II diffractometer and the raw data were corrected for Lorentz and polarization effects. An absorption correction was applied using X-Red [22] and X-Shape [23]. The refinements were done against F^2 employing SHELXL-97 [24]. Technical details of the data acquisition and some selected results of the refinements are summarized in Table 1. All atoms were refined with anisotropic displacement parameters. The final atomic co-ordinates as well as the equivalent isotropic displacement parameters are listed in Table 2. Table 3 shows a comparison of the shortest interatomic distances in the range of 2.5−3.5 Å. Further details of the crystal structure investigations may be obtained from the Fachinformationszentrum Karlsruhe D-76344 Eggenstein-Leopoldshafen, Germany on quoting the depository numbers CSD-418474 (Q=S), CSD-418475 (Q=Se) and CSD-418476 (Q=Te).

d) UV-Vis spectroscopy

For the investigation of the reflectance spectra an UV-VIS-NIR-two-channel spectrometer Cary 5 (Varian Techtron Pty., Darmstadt) was employed. The spectra were transformed into absorption spectra through the Kubelka-Munk function $\alpha/S = (1-R)^2/2R$, (α = absorption coefficient, R = reflectance with given wave length and S = scattering coefficient) [25]. The optical band gap was estimated from the intersection point between the abscissa and the tangent to the linear part of the absorption edge in the plot α/S = f(Eg). $BaSO_4$ powder was used as white standard.

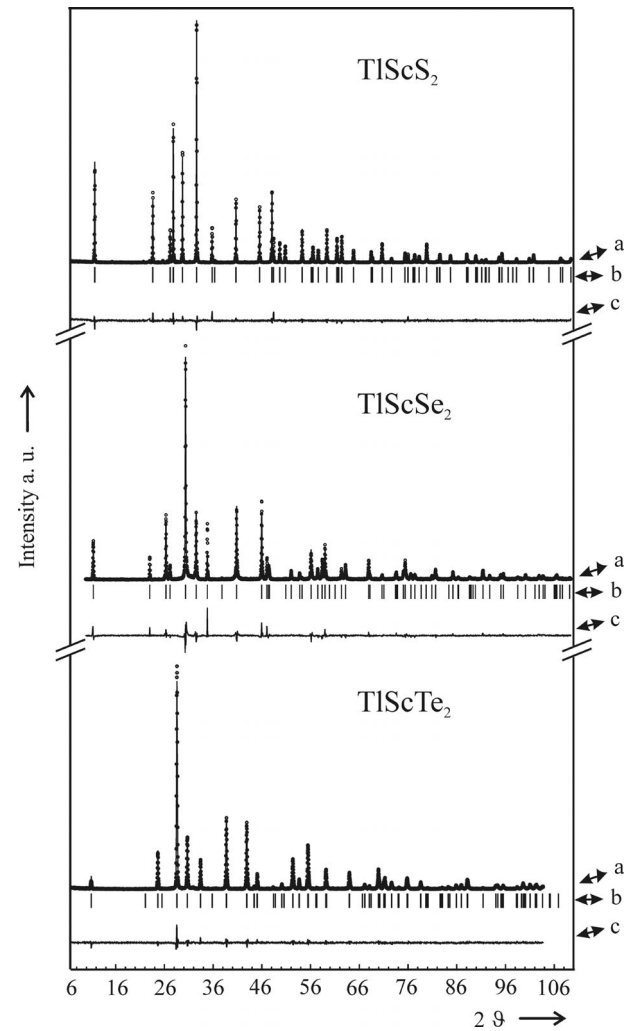

Fig. 1 X-ray powder diffraction patterns of $TlScQ_2$ (Q = S, Se and Te). (a) Circles observed intensities, line calculated intensities, (b) peak positions, (c) I_{obs}-I_{calc}.

e) Band structure calculations

To get a more detailed insight into the electronic structure of the investigated systems, additional calculations have been performed within the local-density approximation to the density functional theory using the relativistic linear-muffin-tin orbital (LMTO) method in the atomic-sphere approximation (ASA) [26]. The von Barth-Hedin [27] exchange-correlation has been used. A cut-off of l_{max} = 3 in decomposition of the wave functions has been used. The Brillouin zone (BZ) integrations were performed using the tetrahedron method on a grid of 189 k-points in 1/12 (irreducible part) of the BZ for $TlScSe_2$ and $TlScTe_2$ and 144 **k**-points in 1/24 (irreducible part) of BZ for $TlScS_2$.

Table 1 Crystal data and structure refinement results for $TlScQ_2$ (standard deviations in parentheses).

Empirical formula	$TlScS_2$	$TlScSe_2$	$TlScTe_2$
Formula weight	313.45	407.25	504.53
Temperature	293(2) K	293(2) K	293(2) K
Crystal system	hexagonal	trigonal	trigonal
Space group	$P6_3/mmc$	$R\bar{3}m$	$R\bar{3}m$
a /Å	3.761(3)	3.9370(4)	4.2129(4)
c /Å	14.942(4)	23.194(5)	24.099(3)
Volume /Å^3	183.0(2)	311.33(8)	370.42(7)
Z	2	3	3
ρ (calcd.) / g cm^{-3}	5.687	6.516	6.785
μ / mm^{-1}	46.683	57.700	45.338
Θ range /°	2.73−30.04	2.63−27.83	2.54−29.95
Reflections collected	540	1152	483
Independent reflections	135	121	171
R_{int}	0.0519	0.1016	0.0699
Refinement method	Full-matrix least-squares on F^2		
Data / parameters	135 / 9	121 / 8	171 / 8
GOF (F^2)	1.122	1.245	1.047
R_1	0.0308	0.0483	0.0478
wR_2	0.0671	0.1215	0.0817
Extinction coefficient	0.014(3)	−	−
δF / e/Å^3	1.823/−1.297	3.203/−2.978	2.260/−1.556

Table 2 Atomic co-ordinates (z × 10^4) and equivalent isotropic displacement parameters (Å$^2 \cdot 10^3$) for $TlScQ_2$. U_{eq} is defined as one third of the trace of the orthogonalized U_{ij} tensor.
In the space group $P6_3/mmc$ (No. 194) the atoms occupy the positions: Tl (2*d*) $\bar{6}m2$, Sc (2*a*) $\bar{3}m$ and S (4*e*) *3m* and in the space group $R\bar{3}m$ (No. 166) Tl (3*b*) $\bar{3}m$, Sc (3*a*) $\bar{3}m$ and Se or Te (6*c*) *3m*, respectively (standard deviations in parentheses).

	$TlScS_2$			
	x	y	z	U(eq)
Tl	1/3	2/3	1/4	31(1)
Sc	0	0	1/2	17(1)
S	1/3	2/3	5947(2)	17(1)
	$TlScSe_2$			
	x	y	z	U(eq)
Tl	0	0	1/2	29(1)
Sc	0	0	0	16(1)
Se	0	0	2683(1)	15(1)
	$TlScTe_2$			
	x	y	z	U(eq)
Tl	0	0	1/2	34(1)
Sc	0	0	0	20(1)
Te	0	0	2652(1)	20(1)

Table 3 Shortest inter atomic distances /Å for $TlScQ_2$ (standard deviations in parentheses).

$TlScS_2$	
Tl-S	3.178(2) (6×)
Sc-S	2.591(2) (6×)
$TlScSe_2$	
Tl-Se	3.2743(15) (6×)
Sc-Se	2.7282(11) (6×)
$TlScTe_2$	
Tl-Te	3.4000(8) (6×)
Sc-Te	2.9341(6) (6×)

Results and Discussion

a) Crystal structures

The X-Ray investigations revealed that $TlScS_2$ adopts the hexagonal β-$RbScO_2$ type structure, while the homologous $TlScSe_2$ and $TlScTe_2$ crystallize in the α-$NaFeO_2$ structure type. In the latter the anions are densely packed and the cations occupy the octahedral voids thus forming ordered alternating layers stacked along [001]. The surrounding of Sc^{3+} is only slightly distorted with all six Sc-Q distances being identical. Interestingly, the Sc-Se bond length is slightly larger than the sum Σ_r of the ionic radii [19] (Sc-Se = 2.728(1) Å, Σ_r = 2.725 Å) whereas the corresponding Sc-Te bond is shorter by about 0.021 Å (Sc-Te = 2.9341(6) Å, Σ_r = 2.955 Å). The angles Q-Sc-Q in the basal planes are in the range from 87.64(5) to 92.36(5)° (Q = Se) and 88.24(2) to 91.76(2)° (Q = Te), respectively. The surrounding of Tl^+ is markedly more distorted. All distances are equal and significantly shorter than the sum of the ionic radii [19] (Tl-Se = 3.274(2), Σ_r = 3.48 Å, Tl-Te = 3.4000(8) Å, Σ_r = 3.71 Å) indicative for a pronounced covalent character of the Tl-Se/Te bonds. The angles Q-Tl-Q in the basal planes range from 73.91(4) to 106.09(4)° for $TlScSe_2$ and are between 76.57(2) and 103.43(2)° for $TlScTe_2$. The structural parameters indicate a slight increase of the distortion within the homologous series $TlScQ_2$ (Q = Te, Se) with decreasing radius of Q^{2-} ($r(Te^{2-})$ = 2.21 and $r(Se^{2-})$ = 1.98 Å [19]). For the sulfide the distortion around Sc^{3+} is similar small with S-Sc-S angles in the range from 86.95(7) to 93.05(7)°. The Sc-S bond length of 2.591(2) Å is longer than the sum of the ionic radii of 2.585 Å. A severe alteration as compared to the Se/Te compounds of the environment around Tl^+ is evident leading to a trigonal prismatic coordination (Fig. 2, left) rather than an octahedral surrounding. Again, the Tl-S bond lengths are shorter than the sum of the ionic radii of Tl^+ and S^{2-} (Tl-S: = 3.1782(2) Å, Σ_r = 3.34 Å). The two opposite triangular faces of the octahedron in the α-$NaFeO_2$ type being perpendicular to [001] are twisted (Fig. 2) to form the two corresponding gable faces of the prism. Hence, the anion layers neighboring to Tl^+ are no longer densely packed along [001] but instead a bcc-type arrangement is realized to suite the space requirement of Tl^+ in a surrounding of the smaller sulfur atoms. In this connection the adopted β-$RbScO_2$ type structure of $TlScS_2$ is very likely to be the high pressure form of the selenide and telluride.

b) Electrical conductivity

The electrical measurement (Fig. 3) revealed that the compounds are semiconductors or poor metals, respectively. $TlScS_2$ behaves like a semiconductor in the temperature region between 130 and 300 K while below T ≈ 102 K the resistivity is decreasing with decreasing temperature. This behavior may indicate a semiconductor to metal transition

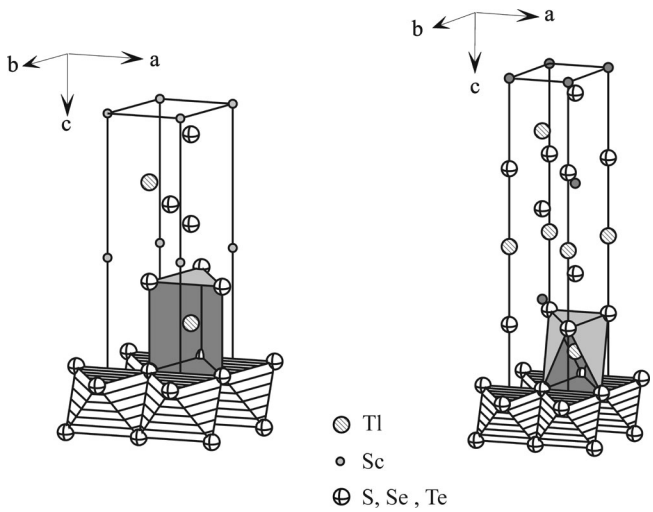

Fig. 2 Crystal structure of $TlScS_2$ (β-$RbScO_2$ type) left and $TlScSe_2$ or $TlScTe_2$, respectively (α-$NaFeO_2$ type) right.

in the low temperature region. The selenide and the telluride behave different with a resistivity of the latter being about two magnitudes lower than that of the former compound. But the temperature dependence of the resistivity of the selenide and the telluride is very similar showing hardly any change of the resistivity with decreasing temperature in the range from 300 to 12 K. There is a very slight increase of the resistivity at low temperatures to be seen better for the telluride (Fig. 3).

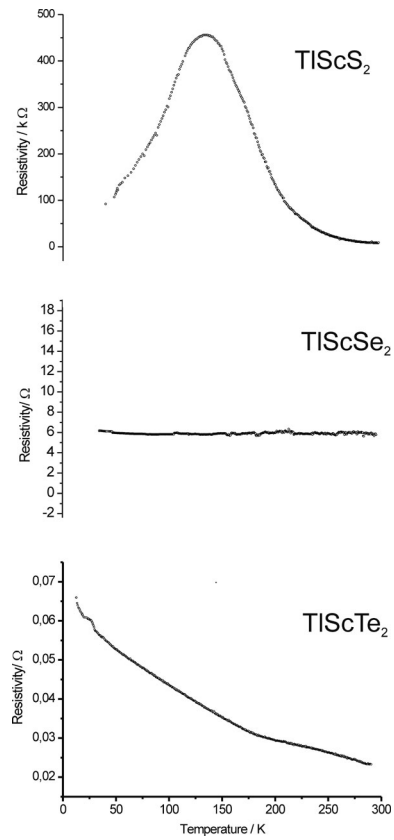

Fig. 3 Resistivity as a function of temperature for $TlScQ_2$ (Q = S, Se and Te).

c) Electronic band structure

The total as well as component and angular momentum resolved density of states (DOS) curves for the three compounds are displayed in Figure 4. As can be seen from the drawings the sulfur and selenium compounds are semiconductors with a very small band gap or they are poor metals, whereas the tellurium compound is calculated to be a metal, but conductivity or spectroscopic investigations suggest that it is a semiconductor. The values for the optical band gaps estimated from reflectance spectra are 1.51 eV for $TlScS_2$ and 0.79 eV and 0.85 eV for $TlScSe_2$ and $TlScTe_2$, respectively. For all three compounds the valence band (VB) between 0 and −5 eV is dominated by hybridized chalcogen *p* and Sc *d* states. An admixture of small contributions of Tl based *s*, *p*, and *d* states is also seen in this region. Within an ionic picture one would expect that Sc based states are empty but according to the calculations there is relatively large contribution of Sc *d* states to the DOS in the VB. The largest contribution in the VB shifts slightly to higher energies from about −3 eV for $TlScS_2$ to −2.3 eV for $TlSTe_2$ in agreement with the alteration of the electronegativity of the chalcogen atoms going from S to Te. In addition, at the bottom of the VB around −6 eV mainly Tl *s* state contributions are located. Interestingly, these Tl *s* states shift to slightly lower energy values and become narrower going from S to Te. In the Te compound this band is separated from the rest of the VB, i.e., it is a semi-core band. From a chemical point of view the Tl $6s^2$ electron lone-pair is part of the VB in $TlScS_2$ and $TlScSe_2$ whereas in the Te compound the lone-pair is fully separated.

In the conduction band (CB) Sc *d* states as well as Tl *p* states are the main components with a minor contribution from Tl *d* states. The DOS of Tl based states in the VB and CB exhibits a more structured shape for $TlScS_2$ than for the other two compounds which may be due to the more covalent character of the bonds in the latter two chalcogenides. The DOS at the Fermi energy (E_F) in $TlScTe_2$ comes from Te based states and Sc *d* states. One explanation may be that Te atoms with the lowest electronegativity donate electrons to empty Sc *d* states.

A detailed picture about the bonding properties is gained from the energy dispersion relation *E*(k). Figure 5 shows the electron energy band structure of the ground states of the compounds. For all compounds the bands exhibit strong dispersions along distinct high symmetry directions reflecting strong bonding interactions between the atoms along these directions. For $TlScS_2$ the top of the VB is located at the Γ point whereas the bottom of the CB is at the M point, i.e., the compound is an indirect semiconductor.

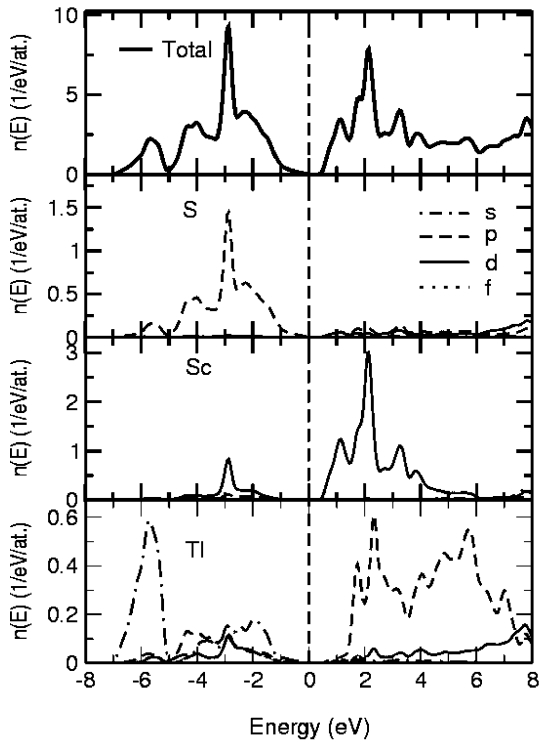

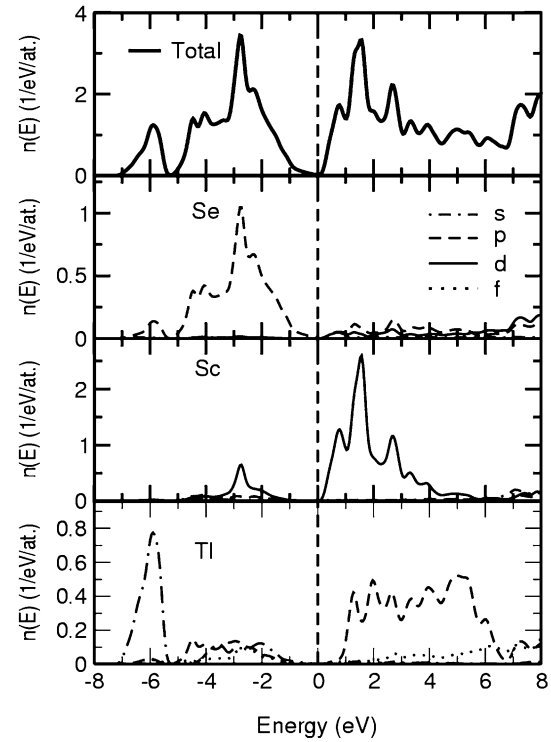

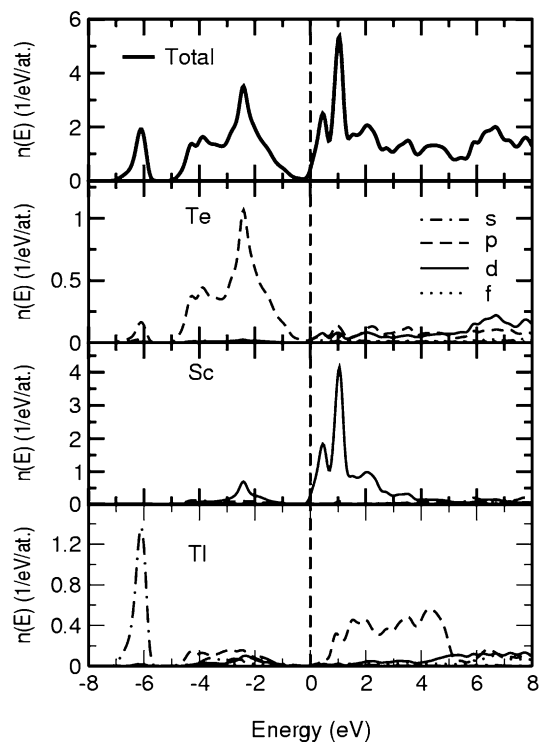

Fig. 4 The density of states curves for $TlScQ_2$ (top: Q = S; middle: Q = Se; bottom: Q = Te).

Parts of the bands along Γ-M, Γ-K and Γ-A are just below E_F, whereas all other bands are lower in energy. A pronounced dispersion of the bands along Γ-M and Γ-K gives clear evidence for strong bonding interactions for the atoms within the a_1-a_2 plane. For the Se compound the top of the VB is located at the Z point and the bottom of the CB at U_N. Hence, this compound is also an indirect semiconductor. Strong dispersions are found along Γ-Z and Z-U_N which is caused by strong bonding interactions, especially between Sc and Se. Finally, the dispersion relation for $TlScTe_2$ is very similar to that of the Se compound. The main difference is that the bands along Γ-Z and Z-U_N now cross the Fermi level, i.e., the calculations suggest that this compound should be a metal.

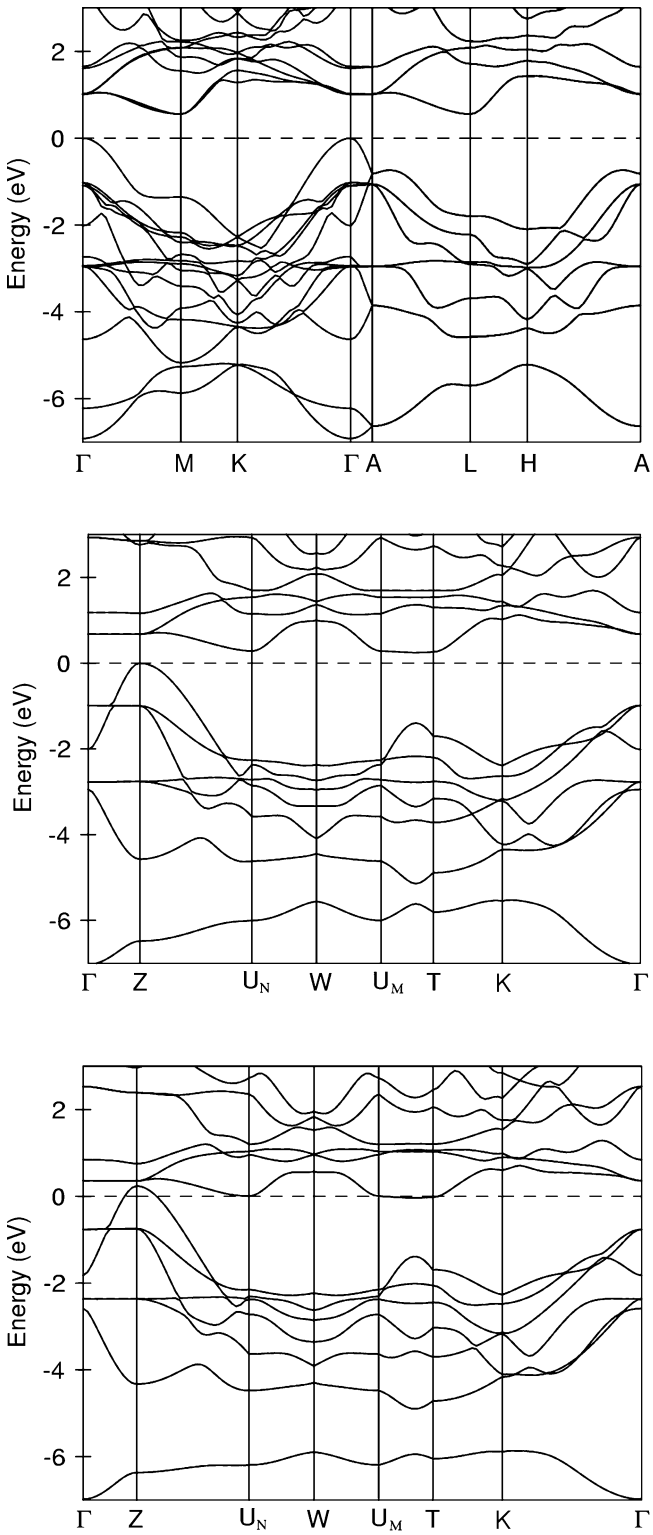

Fig. 5 The E(k) relations for $TlScQ_2$ (top: Q = S; middle: Q = Se; bottom: Q = Te).

Conclusions

The homologous series $TlScQ_2$ (Q= S, Se and Te) was prepared and the crystal structures were determined. For Q = S the β-$RbScO_2$ type structure is adopted, while the selenide and the telluride crystallize in the α-$NaFeO_2$ type. This observation is explained applying the rough relation between chemical composition, atomic volume and possible crystal structures. Hence, the substitution of Se or Te for S is accompanied by a reduction of the partial molar volume and this may be viewed as an increase of the so-called "chemical pressure". The latter may be responsible for a distortion of the polyhedron around Tl^+ and for stabilising the β-$RbScO_2$ type structure. The physical measurements indicate that the new compounds are semiconductors or poor metals. According to the electronic band structure calculations $TlScS_2$ and $TlScSe_2$ are semiconductors with small band gaps whereas the telluride should be a metal. The contradiction between the experimental findings and the results of the theoretical work is not surprising, because it is well known that DFT based methods underestimate the value for the electronic band gap. One should also keep in mind that the resistivity measurements were performed on pressed pellets and grain boundary effects may affect the experimental values. Nevertheless, the results of the band structure calculations yield a detailed picture of the bonding situation. As expected the covalent character of the bonds increases from S to Te, being in accordance with the decreasing electronegativity going from S via Se to Te. In the same direction the metallic character of the homologous compounds increases. It is a challenging task to prove experimentally that $TlScSe_2$ and $TlScTe_2$ can adopt the β-$RbScO_2$ type structure under high pressure conditions as suggested by the results of the present work. If this transition can be experimentally realized it is of great interest to learn more about the pressure dependent behavior of the electronic states applying appropriate band structure calculations. The temperature dependence of the resistivity of $TlScS_2$ requires low temperature X-ray diffraction experiments which may show whether the transition from typical semiconductor to a metallic like behavior is accompanied by a structural phase transition.

References

[1] R. Ballestracci, E. F. Bertaut, *Bull. Soc. Fr. Miner. Cristall.* **1964**, *87*, 512.
[2] R. Ballestracci, *Bull. Soc. Fr. Miner. Cristall.* **1965**, *88*, 207.
[3] T. Ohtani, H. Honjo, H. Wada, *Mater. Res. Bull.* **1987**, *22*, 829.
[4] T. Schleid, F. Lissner, *Eur. J. Solid State Inorg. Chem.* **1993**, *30*, 829.
[5] M. Sato, G. Y. Adachi, J. Shiokawa, *Mater. Res. Bull.* **1984**, *19*, 1215.
[6] M. Sato, G. Y. Adachi, J. Shiokawa, *Bull. Soc. Fr. Miner. Cristall.* **1984**, *87*, 512.
[7] W. Bronger, R. Elter, E. Maus, T. Schmitt, *Rev. Chim. Miner.* **1973**, *10(1-2)*, 147.
[8] W. Bronger, W. Brueggemann, M. von der Ahe, D. J. Schmitz, *Alloys Compd.* **1993**, *200*, 205.
[9] W. Bronger, J. Eyck, K. Kruse, D. Schmitz, *Eur. J. Solid State Inorg. Chem.* **1996**, *33*, 213.

[10] C. Plug, G. C. Verschoor, *Acta Crystallogr.* **1976**, *B32*, 1856.
[11] C. Plug, G. C. Verschoor, *Bull. Soc. Fr. Miner. Cristall*. **1976**, *88*, 207.
[12] P. M. Keane, J. A. Ibers, *Acta Crystallogr*. **1992**, *C48*, 1301.
[13] B. Deng, D. E. Ellis, J. A. Ibers, *Inorg. Chem*. **2002**, *41*, 5716.
[14] K. Stöwe, C. Napoli, S. Appel, *Z. Anorg. Allg. Chem*. **2003**, *629*, 1925.
[15] A. K. Gray, B. R. Martin, P. K. Dorhout, *Z. Kristallogr., New Cryst. Struct.* **2003**, *218*, 20.
[16] B. Deng, J. A. Ibers, *Acta. Crystallogr.* **2005**, *E 61*, i15.
[17] F. Lissner, T. Schleid, *Z. Anorg. Allg. Chem.* **2003**, *629*, 1895.
[18] H. Wiench, G. Brachtel, R. Hoppe, *Z. Anorg. Allg. Chem.* **1977**, *436*, 169.
[19] R. D. Shannon, *Acta Crystallogr.* **1976**, *A 32*, 751.
[20] C. L. Teske, W. Bensch, *Z. Anorg. Allg. Chem.* **2002**, *628*, 1511.
[21] L. J. Van der Pauw, *Phillips Res. Rept*. **1958**, *13*, 1; J. P. Suchet, Electrical Conduction in Solid Materials, Pergamon Press Oxford **1975**.
[22] X-RED, Data Reduction Program, Version 1.11, Stoe Cie, **1998**.
[23] X-SHAPE, Version 1.03, Stoe & Cie, Darmstadt, Germany, **1998**.
[24] G. M. Sheldrick, SHELXL-97, *A Program Package for the Solution and Refinement of Crystal Structures*, Univ. Göttingen, Germany **1997**.
[25] P. Kubelka, F. Munk, *Z. Tech. Phys.* **1931**, *12*, 593.
[26] O. Andersen, *Phys. Rev.* **1975**, *B 12*, 3060.
[27] U. von Barth, L. Hedin, *J. Phys.* **1972**, *C 51*, 629.

